Investigation of the Cold-Start Combustion Characteristics of Ethanol−Gasoline Blends in a Constant-Volume Chamber

ARTICLE *in* ENERGY & FUELS · MARCH 2005

Impact Factor: 2.79 · DOI: 10.1021/ef049733l

5 AUTHORS, INCLUDING:

Shiyong Liao
Xi'an Jiaotong University
26 PUBLICATIONS **377** CITATIONS
SEE PROFILE

Zuohua Huang
Xi'an Jiaotong University
421 PUBLICATIONS **5,195** CITATIONS
SEE PROFILE

Investigation of the Cold-Start Combustion Characteristics of Ethanol−Gasoline Blends in a Constant-Volume Chamber

S. Y. Liao,*,†,§ D. M. Jiang,† Q. Cheng,‡ Z. H. Huang,† and Q. Wei†

School of Energy and Power Engineering, Xi'an Jiaotong University, Xi'an 710049, People's Republic of China, and College of Chongqing Communication, Chongqing 400035, People's Republic of China

Received October 25, 2004. Revised Manuscript Received February 14, 2005

This experimental study conducted in a closed combustion chamber is to investigate combustion characteristics of ethanol−gasoline blends at low temperature, which is related to the cold-start operation of engines fueled with ethanol−gasoline. It presents the effects of the fuel amount injected into the combustion vessel on the combustion process, and some key characteristic parameters, such as ignition delay time, mass burning rate, and flame speeds, have been explored. The result shows that, for an ethanol−gasoline engine, it must not be overfueled to realize a reliable cold start, as is the case for a gasoline engine at the same temperature, especially at a temperature range around ethanol's boiling point, because ethanol addition into gasoline results in the improvement of blend evaporation. Moreover, The exhaust emissions are purposely measured in terms of unburned hydrocarbon (HC), carbon monoxide (CO), and oxides of nitrogen (NOx) emissions. It is confirmed that the emissions of HC during rich combustion at relative low temperature should be increased with the increasing addition of ethanol into gasoline, but at separated optimization equivalence ratio for cold start, HC and CO emissions can be obviously reduced. The flame speeds are investigated as well. It is shown that, for ethanol−gasoline blends with ethanol content below 30%, the suitable fuel−air ratio to realize fast flame propagation is about 1.3.

Introduction

The increasing demand for energy and stringent pollution regulations, as a result of the population growth and technological development in the world, promote research on alternative fuels. Ethanol is a clear, colorless liquid that can be made from a variety of sources including sugar cane and maize. Ethanol has been identified as having the potential to improve air quality when used to replace conventional gasoline in engines because of its good anti-knock characteristics and the reduction of CO and unburned hydrocarbon (HC) emissions.[1] Certainly, the use of ethanol is also accompanied with a disadvantage of increase in aldehyde and unburned ethanol emissions. Moreover, ethanol proponents have also typically focused on the renewable characteristics, presenting the benefits of ethanol in terms of local energy security and stabilization of the agricultural sector.[2] Thereby, ethanol is being regarded as one of the promising alternative fuels for engines.

It is well known that ethanol has a greater heat of vaporization than gasoline; more ethanol addition into gasoline can make the cold-start worse due to the lower in-cylinder temperature. Thereby, fuels with a lower ethanol content are mainly promoted in practical engine utilization, such as gasohol, containing 10% ethanol volume fraction, used in North America, reformulated gasoline containing 7.6% (v/v) ethanol, popularized in the USA.[3] Moreover, Brazil, as a lead country in ethanol production, has approved an increase in ethanol content in gasoline even beyond 26%.[3] Generally, ethanol fuel is designated E100 to identify it as essentially 100% pure ethanol and a popularly used ethanol blend composed of 15% ethanol and 85% unleaded gasoline is designated as E15.

In view of environmental protection, a major difficulty in meeting rigorous emissions standards is the initial cold-start transient, where the HCs emitted remain at a high level because of the richer fuel−air mixture supplied, as well as the lower efficiency of catalytic converter.[4] It has been suggested that a significant reduction in cold-start HC emissions could be obtained by operating the engine at a near-stoichiometric ratio or preferably slightly leaner than stoichiometric where the HC emissions are at a minimum. However, there are some significant difficulties in achieving this goal

* Author to whom correspondence should be addressed. E-mail: shyliao@yahoo.com.cn.
† Xi'an Jiaotong University.
‡ College of Chongqing Communication.
§ Current address: College of Chongqing Communication, Chongqing 400035, PRC.

(1) Moreira, J. R.; Goldemberg, J. The Alcohol Program. *Energy Policy* **1999**, *27*, 229−245.
(2) Thomas, V.; Kwong, A. Ethanol as a lead replacement: phasing out leaded gasoline in Africa. *Energy Policy* **2001**, *29*, 1133−1143.
(3) Nadim, F.; Zack, P.; Hoag, G. E., Liu, S. L. United States experience with gasoline additives. *Energy Policy* **2001**, *29*, 1−5.
(4) Henein, N. A.; Tagomori, M. K. Cold-start hydrocarbon emissions in port-injected gasoline engines. *Prog. Energy Combust. Sci* **1999**, *25*, 563−593.

10.1021/ef049733l CCC: $30.25
Published on Web 03/16/2005

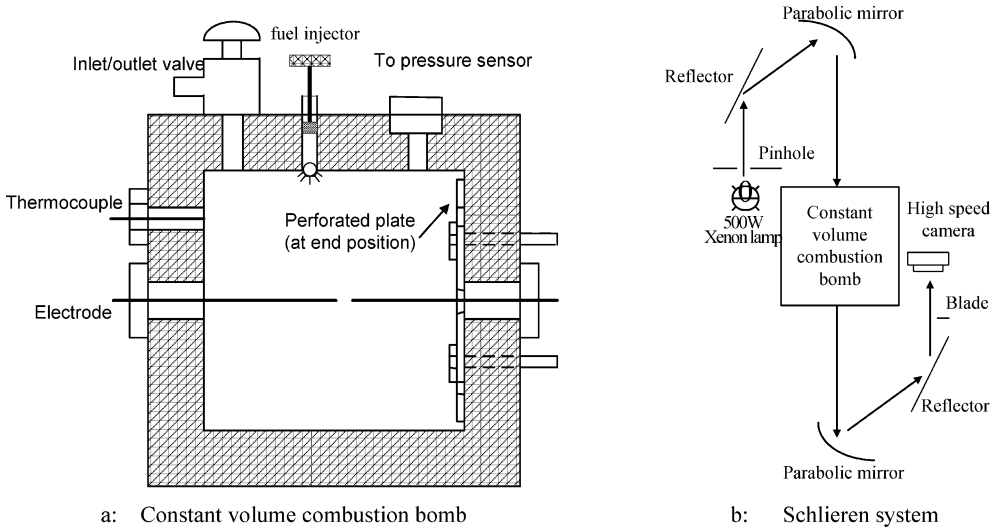

Figure 1. Schematic diagram of the experimental system.

for cold-start transients of spark ignition (SI) engines. One of the most difficult problems is that the engine must be overfueled to compensate for liquid fuel accumulation in the intake port walls and cylinder such that the fuel/air ratio in the gas phase is near stoichiometric. Thus, to obtain lower HC emission levels and realize reliable operation, the cold-start combustion process should be well addressed.

For ethanol−gasoline blend engines, the previously reported work was mainly focused on the engine tests related to thermal efficiency, power output, and emissions characteristics.[5−9] Few works can be found in the fundamental aspect of the combustion characteristics of ethanol−gasoline blended fuels at low temperature. From these considerations above, the main objective of this study is to explore the possibility of rapid and reliable cold-starts for the use of ethanol-gasoline blends. As temperature is the leading parameter affecting the formation of fuel−air mixture, it is hence discussed in detailed herein. Mixtures with various equivalence ratios are ignited centrally in a combustion bomb to investigate the combustion process and flame-propagation characteristics for ethanol, gasoline, and blended fuels of E15 and E30.

Experimental Methods

Idealized engine combustion studies, conducted in a constant-volume combustion bomb, can be used to simulate engine combustion process near the top dead center at the end of the compression stroke. Shown in Figure 1 are the schematic diagrams of the combustion bomb and the optical system used for recording the flame growth. The combustion bomb has an inside size of 108 × 108 × 135 mm^3, as shown in Figure 1a. Two sides of this bomb are transparent to make the inside observable; these sides are to provide the optical access, and the other four sides are enclosed with resistance coils to heat the bomb to the desired preheat temperature. The inlet/outlet valve is used to let fresh air or combustion product in or out. The liquid fuel needed is precalculated corresponding to the given equivalence ratio, and it is then injected into the combustion chamber using a small capability injector. The function of the motion of the perforated plate is to simulate the airflow in the engine intake port to enhance the fuel's evaporation. Two extended stainless-steel electrodes are used to form the spark gap at the center of this bomb. A conventional battery-coil ignition system is used for producing the spark. The history of the shape and size of the developing flame kernel is recorded by a high-speed camera (NEC E-10) operating at 5000 pictures per second with a schlieren optical system, and the detailed experimental setup about the schlieren system is given in Figure 1b. Dynamic pressure is measured since spark ignition with a piezoelectric absolute pressure transducer, model Kistler 4075A, with a calibrating element Kistler 4618A. The AVL Di Gas4000 emissions analyzer is used to measure the concentration of NOx, HC, and CO.

The films are processed on a film analyzer (NEC Model 100).[10] First, the flames in the film are projected and enlarged on a screen; then, the schlieren flame contours are manually traced, and a microcomputer is used to assemble the location information of these points. From the surface enclosed by the contours, the flame size can be determined. This technique was used previously by Shen and Jiang[10] and Tagalian and Heywood.[11]

Combustion Analysis and Flame Speed. To extract information on the combustion process, a cycle-resolved mass burning rate calculation is performed using a quasi-dimensional two-zone combustion model. Assuming the flame front is a thin, reactive sheet, the model divides the combustion chamber into two zones, i.e., burned zone and unburned zone, and is based on the following assumptions:

1. The mixture will be burned immediately after entering the flame region.

2. The burned gas within the flame kernel is in chemical equilibrium.

(5) Hasan, M. A. Effect of ethanol-unleaded gasoline blends on engine performance and exhaust emission. *Energy Convers. Manage.* **2003**, *44*, 1547−1561.

(6) Yuksel, F.; Yuksel, B. The use of ethanol-gasoline blend as a fuel in an SI engine. *Renewable Energy* **2004**, *29*, 1181−1191.

(7) Schifter, I.; Diaz, L.; Vera, M.; Guzman, E.; Lopez. S. E. Fuel formulation and vehicle exhaust emissions in Mexico. *Fuel* **2004**, *83*, 2065−2074.

(8) Poulopoulos, S. G.; Samaras, D. P.; Philippopoulos, C. J. Regulated and unregulated emissions from an internal combustion engine operating on ethanol-containing fuels. *Atmospheric Environment* **2001**, *35*, 4399−4406.

(9) Ulmera, J. D.; Huhnkeb, R. L.; Bellmerc, D. D.; Cartmelld, D. D. Acceptance of ethanol-blended gasoline in Oklahoma. *Biomass Bioenergy* **2004**, *27*, 437−444.

(10) Shen, H. X.; Jiang, D. M. Investigation on the flame initiation and early development in a spark ignition engine. SAE Paper 922239, 1992.

(11) Tagalian, J.; Heywood, J. B. Flame initiation in a spark ignition engine. *Combust. Flame* **1986**, *64*, 243−246.

3. The pressure is uniform throughout the burned and unburned zone.

Then, the mass and energy conservation yield

$$\frac{dm_b}{dt} + \frac{dm_u}{dt} = 0 \quad (1)$$

$$\frac{d(mu)_k}{dt} + p\frac{dV_k}{dt} - \frac{dm_k}{dt}h_k = \frac{dQ_k}{dt} \quad (k = u,b) \quad (2)$$

and from the combined equations of state

$$pV_k = m_k R_k T_k \quad (k = u,b) \quad (3)$$

The following equations can be obtained from ref 11

$$\frac{dT_u}{dt} = \frac{1}{m_u c_{pu}}\left(V_u\frac{dp}{dt} + \frac{dQ_u}{dt}\right) \quad (4)$$

$$\frac{dT_b}{dt} = \frac{1}{m_b R_b}\left[p\frac{dV}{dt} - (R_b T_b - R_u T_u)\frac{dm_b}{dt} - \frac{R_u}{c_{pu}}\left(V_u\frac{dp}{dt} + \frac{dQ_u}{dt}\right) + V\frac{dp}{dt}\right] \quad (5)$$

$$- \left[(u_b - u_u) - c_{vb}\left(T_b - T_u\frac{R_u}{R_b}\right)\right]\frac{dm_b}{dt} -$$

$$\frac{dp}{dt} = \frac{\left(\frac{c_{vu}}{c_{pu}} - \frac{c_{vb}}{c_{pu}}\frac{R_u}{R_b}\right)\frac{dQ_u}{dt} + \left(\frac{dQ_u}{dt} + \frac{dQ_b}{dt}\right)}{V_u\left(\frac{c_{vu}}{c_{pu}} - \frac{c_{vb}}{c_{pu}}\frac{R_u}{R_b}\right) + V\frac{c_{vb}}{R_b}} \quad (6)$$

where the heat losses dQ_u/dt and dQ_b/dt are estimated from Annand's formulas.[12] The mass burning rate $dm_b/dt(\dot{m}_b)$ can then be solved numerically with a fourth-order Runge−Kutta scheme for eqs 4−6. To give a quantitative analysis of flame initialization, the ignition delay time is explored, defined as the time interval from the ignition beginning to the ending timing of 10% mass burned, hence, also named as 10%MFBT herein.

The schlieren system is used to visualize the expanding flames. The stretched flame speed can be well defined as the increased rate of flame size, i.e.,

$$S_n = \frac{dr_u}{dt} \quad (7)$$

From the definition of the flame stretch, α, of a flame front in a quiescent mixture is given by,

$$\alpha = \frac{1}{A}\frac{dA}{dt} \quad (8)$$

where A is the area of flame. Thereby, as to a spherically outwardly expanding flame front, the flame stretch is well defined as,

$$\alpha = \frac{1}{A}\frac{dA}{dt} = \frac{2}{r_u}\frac{dr_u}{dt} = \frac{2}{r_u}S_n \quad (9)$$

As described in refs 13−15, From the linear relationship between flame speeds and the total stretch rates, as eq 10

$$S_l - S_n = L_b\alpha \quad (10)$$

(12) Liao, S. Y.; Jiang, D. M.; Gao, J.; Zeng, K. Effects of different frequency component in turbulence on accelerating turbulent premixed combustion. *Proc. Inst. Mech. Eng., Part D* **2003**, *217*, 1023−1030.

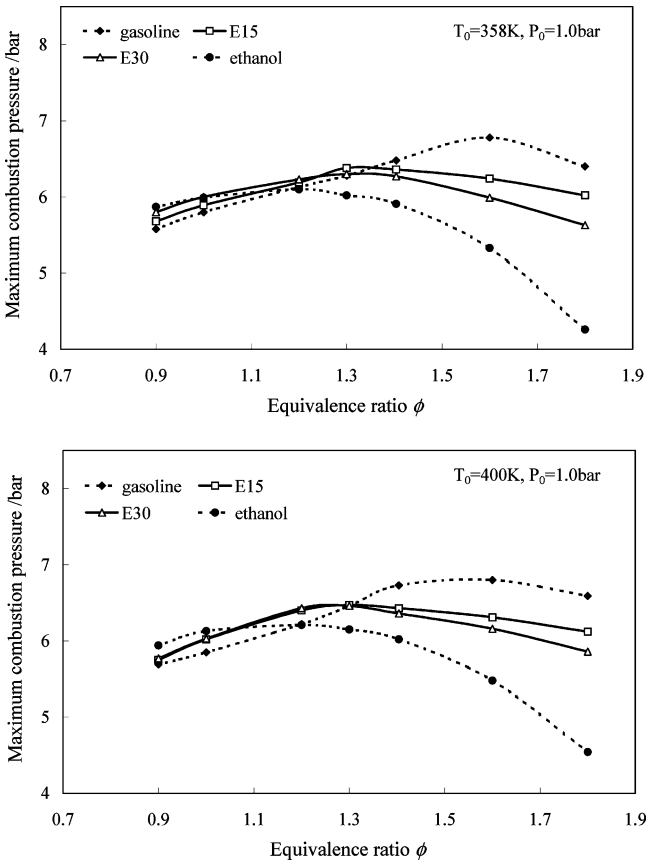

Figure 2. Maximum combustion pressure for various fuels.

Namely, the unstretched flame speed, S_l, can be obtained as the intercept value at $\alpha = 0$ in the plot of S_n against α.

Results and Discussions

Figure 2 plots the peak pressure rise due to combustion for various fuels**.** Here it must be noted that the following equivalence ratio is considered to be the ratio of the fuel injected into chamber to the air, as it is difficult to evaluate the actual fuel amount vaporized because of the complexity of gasoline components. It can be see that the equivalence ratios corresponding to the peak of the maximum combustion pressures are different, and it is obvious that this equivalence ratio of blended fuels (E15 and E30) is about 1.3, less than that of gasoline (about 1.6). It is known that the maximum combustion pressure is strongly related to the amount of the fuel evaporated. Since the evaporation pressures for liquid fuels are mainly dependent on the preheated temperature, it is understandable that these equivalence ratios of E15, E30, and gasoline are bigger than unity because of these fuels being partially evaporated at these tested temperatures.

As the normalized apparent mass burning rate has a very significant importance on the pressure−rise rate related with the NOx emissions, burning rate analysis

(13) Liao, S. Y.; Jiang, D. M.; Gao, J.; Huang, Z. H. Measurement of Markstein numbers and laminar burning velocities for natural gas-air mixtures. *Energy Fuels* **2004**, *18*, 316−326.

(14) Gu, X. J.; Haq, M. Z.; Lawes, M.; Woolley, R. Laminar burning velocity and Markstein lengths of methane-air mixtures. *Combust. Flame* **2000**, *121*, 41−58.

(15) Liao, S. Y.; Jiang, D. M.; Gao, J.; Huang, Z. H.; Cheng, Q. Measurement of Markstein numbers and laminar burning velocities for liquefied petroleum gas-air mixtures. *Fuel* **2004**, *83*, 1281−1288.

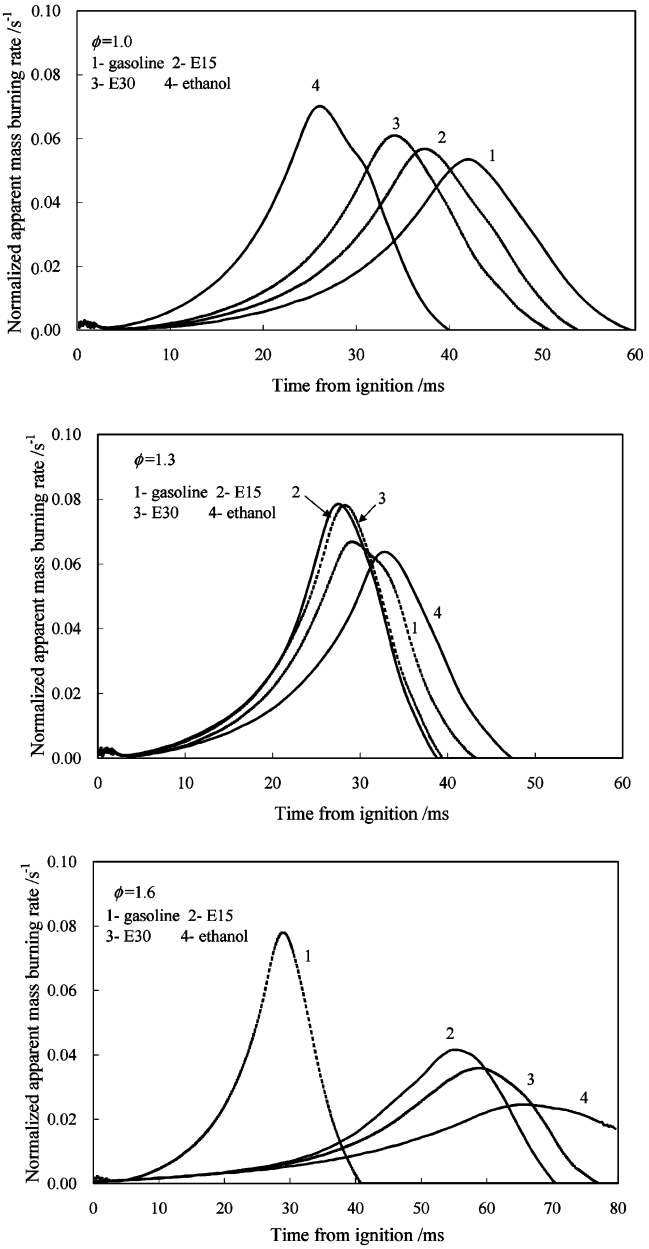

Figure 3. Comparisons of normalized apparent mass burning rates for various fuels at different equivalence ratios, where the initial conditions are 0.1 MPa and 358 K.

is hence used to analyze the combustion process in the chamber. Figure 3 shows the normalized apparent mass burning rates for various fuels at a given temperature of 358 K. As indicated in this figure, the normalized apparent mass burning rate is the main relevant parameter of the fuel−air ratio. Over the presented results, the biggest difference can be found for fuel−air mixtures with an equivalence ratio of 1.6, and the most-likely behaviors are located at an equivalence ratio of 1.3.

The ignition delay time (10%MFBT) is proposed to quantitatively describe the ignitability of fuel−air mixture in this work. Shown in Figure 4 are the variations of ignition delay time (10%MFBT) for various fuels at different equivalence ratios. Obviously, the addition of ethanol content has an important influence on the early flame initialization, as it is indicated that the blended fuel and ethanol show semblable behaviors in ignition

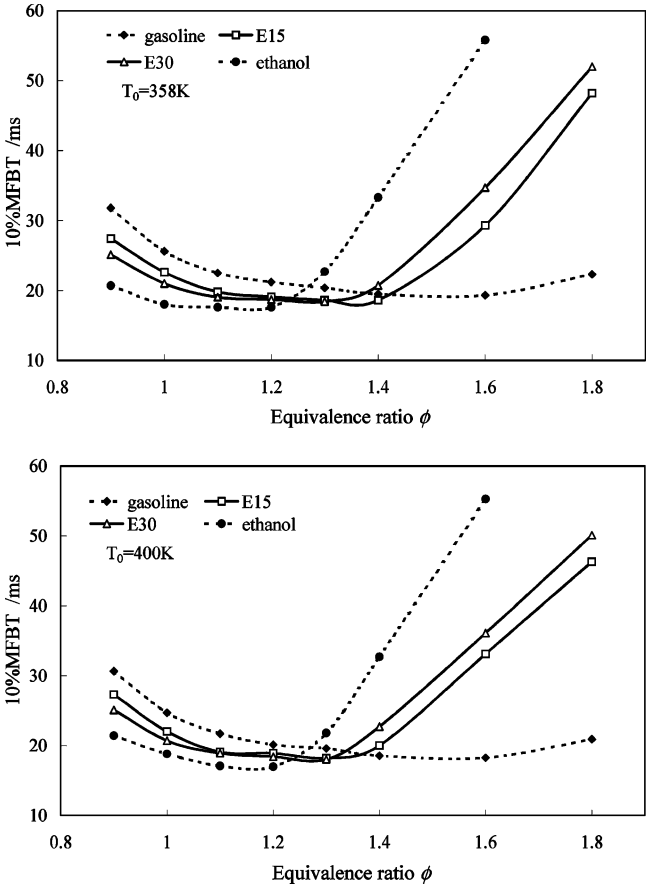

Figure 4. Ignition delay time for various fuels at different equivalence ratios.

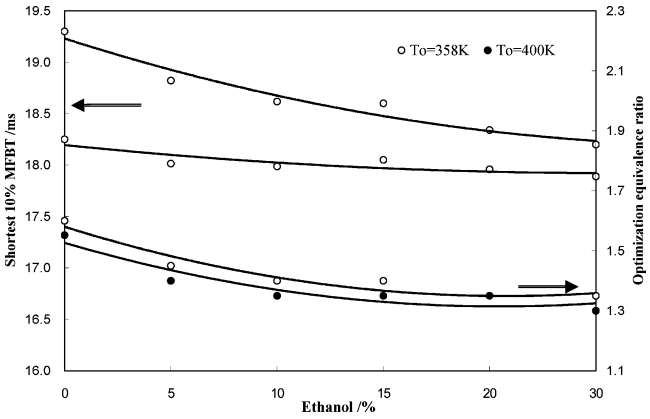

Figure 5. Variations of the shortest 10%MFBT and the optimization equivalence ratio with the increasing ethanol volume fraction.

delay time. Whereas, it is also shown that the minimum value of 10%MFBT for blended fuels has comparable values quantitatively, and the equivalence ratio corresponding to this minimum 10%MFBT is relatively less than that of gasoline. Generally, we think that the shorter ignition delay time indicates a rapid cold start. Thus, for giving a convenient discussion, this equivalence ratio is then defined as the optimization equivalence ratio related to a cold start.

Figure 5 summarizes the effect of ethanol volume fraction on the shortest 10% MFBT of fuel at different preheated temperatures, and the optimization equivalence ratios for different blends are plotted as well. It reports that moderate ethanol addition can result in

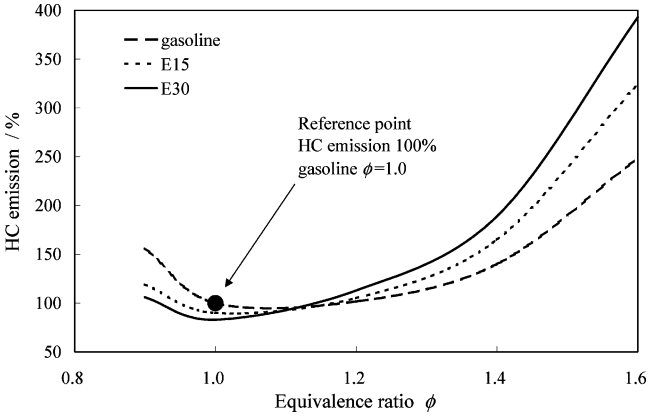

Figure 6. HC emissions for various fuels against the equivalence ratio at 358 K. The reference point is a gasoline−air mixture (ϕ = 1.0) whose HC emission is 100%.

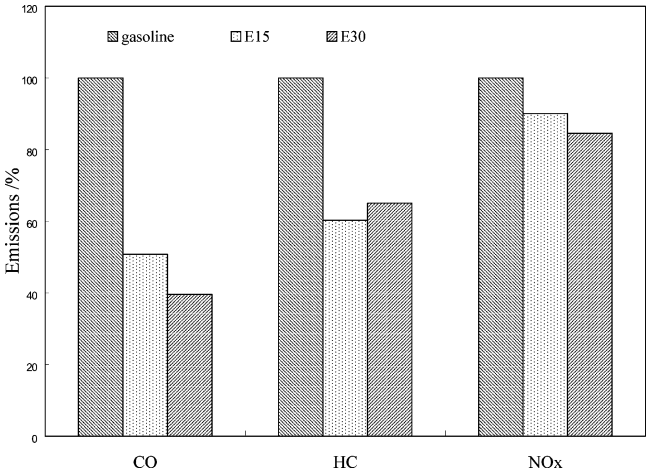

Figure 7. Variations in HC, CO, and NOx emissions for various fuels at the optimization equivalence ratio for a cold start. The reference fuel is gasoline; gasoline emissions are 100%.

obvious shortening of ignition delay time at 358 K. Whereas, with the increase of ethanol content, this phenomenon is not clear and neither are the behaviors of the optimization equivalence ratio of injected fuel to air, which maybe can be explained by the negative effect of the slow flame speed of ethanol becoming obvious. The reduction of ignition delay time with the increase of preheated temperature is also illustrated in this figure. Because the chemical kinetics and the evaporation of fuel are temperature-dependent parameters, it is expected that the ignition delay time and the optimization equivalence ratio decreases with the increase of preheated temperature. However, at 400 K, the curve of 10%MFBT is relatively flat with the increasing of ethanol content, compared to that at 358 K, which is due to the enhancement in evaporation of ethanol addition into gasoline being much more obvious when the preheated temperature is close to ethanol's boiling point (about 350 K).[16]

The effects of ethanol addition on the pollution emissions are studied as well. The experimental measurement is conducted in terms of HC, CO, and NOx emissions at 358 K. Shown in Figure 6 are the HC emissions for various fuels. As ethanol is in full gasification at 358 K, we can see that the addition of ethanol has led to a significant increase of HC emissions through fuel evaporation for rich fuel mixtures. However, from the view of a rapid cold start, the ethanol addition into gasoline also results in the reduction of HC and CO emissions. Figure 7 plots the pollution emissions at the optimization equivalence ratio for a cold start. Obviously, because of the enhance of evaporation, in turn, the fuel injected into chamber decreases; consequently, the HC and CO emissions can be reduced.

Moreover, the flame-propagation characteristics are also discussed in the present work. Shown in Figure 8 is a typical flame kernel growth, and partial measurement results of flame size against the elapsed time are plotted in Figure 9. As mentioned above, from the measurement for these expanding flame kernels, the stretched flame speed can be well induced, as plotted in Figure 10.

Generally, it is indicated that the stretched flame speeds commonly have a lower initialization and gradually increase to a stabilized growth period because of the relatively higher flame stretch and heat loss during the early stage of the flame propagation.[14,15] As mentioned above, the flame stretch is well defined for outward expanding flame; thereby, we can plot the stretched flame speed against flame stretch rate to induce the unstretched flame speed, as in eq 10. Figure 11 plots the results. At stoichiometric conditions (where it is not the actual stoichiometry), the mixture of ethanol−air has the fastest flame speed and, conversely, mixtures of E15, E30, and gasoline in air. While it is a reverse tendency at a richer case (ϕ = 1.6), E15 shows the fastest flame propagation and, conversely, E30 when fuel−air ratio is 1.3. Generally, at high rates of stretch

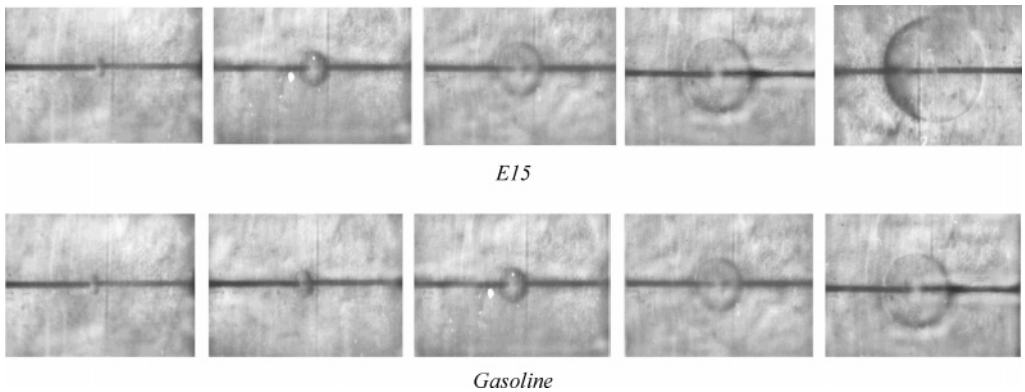

Figure 8. Typical growing schlieren flame kernels for stoichiometric mixtures of E15 and gasoline in air. The time interval is 4 ms; the initial conditions are 0.1 MPa and 358 K.

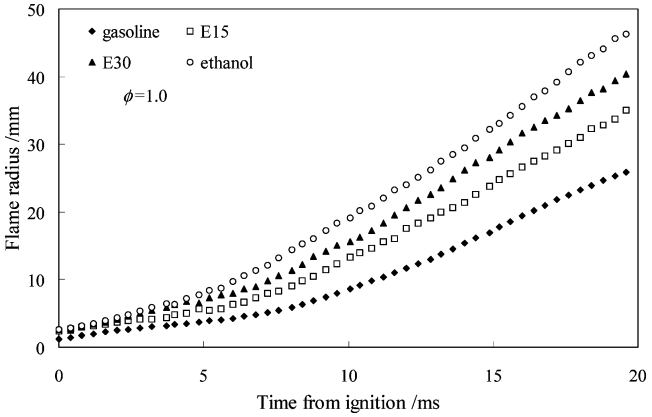

Figure 9. Typical flame growths for a stoichiometric mixture of various fuels in air, where the initial conditions are 0.1 MPa and 358 K.

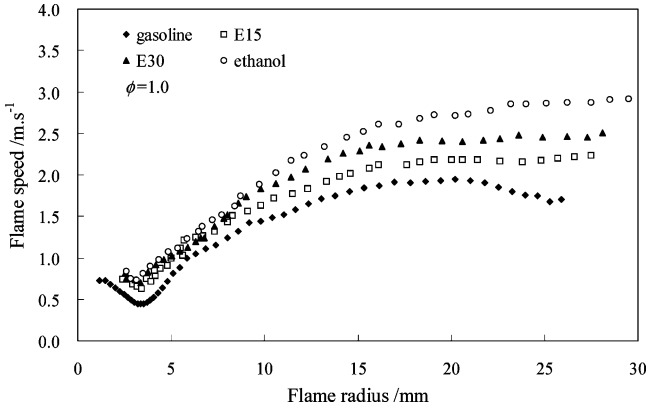

Figure 10. Typical stretched flame speeds for various fuels in air, where the initial conditions are 0.1 MPa and 358 K.

(small flame radius), the flame speed is small, and with the expanding of flame, the flame speed slowly increase due to the reduced flame stretch. As reported previously,[13−15] the ignition energy, initial temperature, and pressure have a strong influence on the flame propagation. Therefore, the flames, restricted within the range in which spark, temperature, and pressure effects can be discounted, are used to induce unstretched flame speed, as indicated in Figure 12. The unstretched flame speeds are plotted in Figure 13. From this figure, it also can be found that the ideal fuel−air ratio of E15 and E30 for 358 K combustion is about at an equivalence ratio of 1.3, and their flame speeds are bigger than those of pure ethanol and gasoline at the same equivalence ratio.

Conclusions

A reliable and rapid cold start of spark ignition engines is related to unburned hydrocarbon emissions, as well as energy efficiency. An experimental investigation on the cold-start combustion characteristics has thus been made in a constant-volume combustion bomb for ethanol−gasoline blended fuels, as combustion characteristics are relevant parameters for a stable combustion initialization. The effect of the equivalence ratio on

(16) He, X. L.; Zhan, Y. H.; Li, S. S. *Fuels applied in internal combustion engines*; Press of Petroleum and Chemistry Industry of China: Beijing, China, 1992.

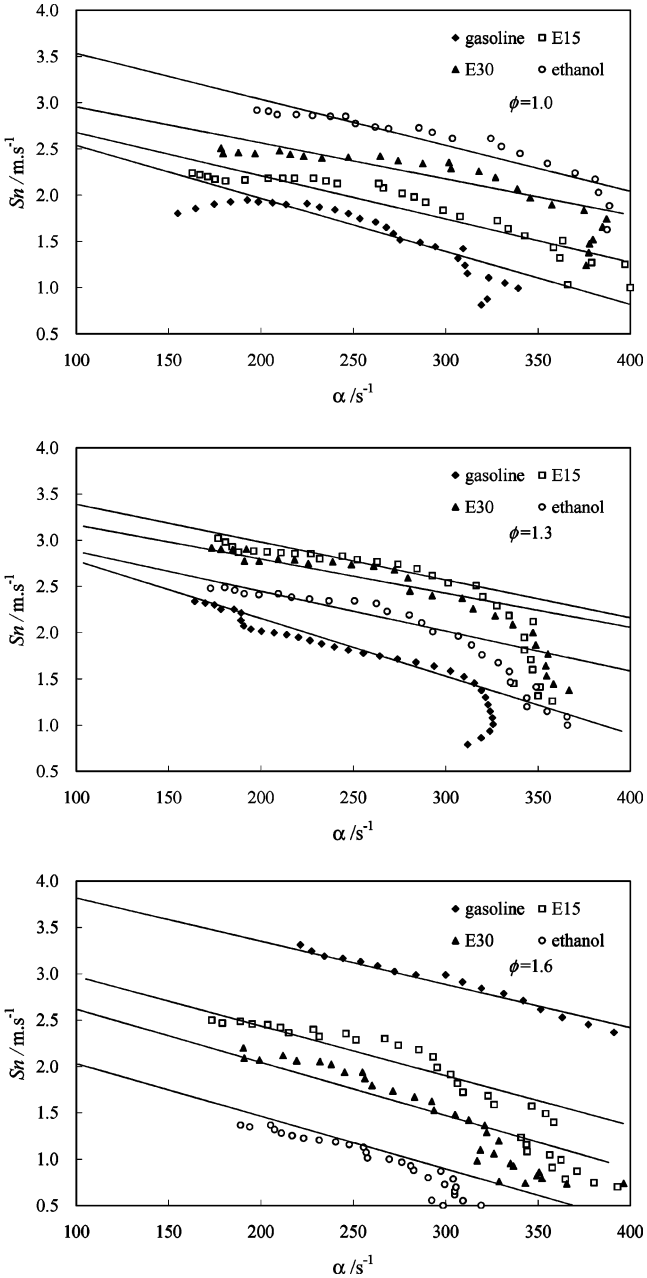

Figure 11. Variations of flame speeds with different stretch rates. The lines are first-order fits through experimental data within the stretch rate (flame radius) range in which spark, temperature, and pressure effects are discounted.

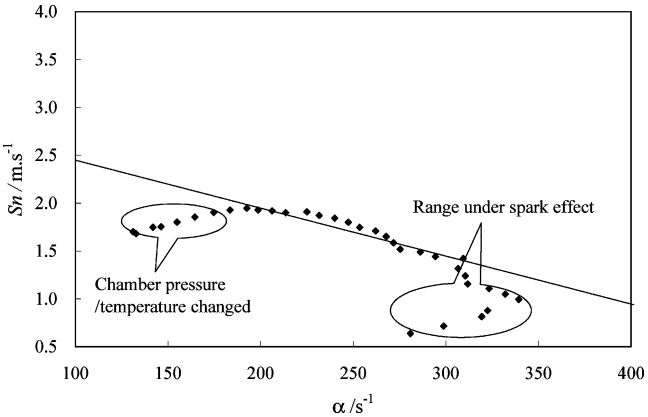

Figure 12. Flame ranges to determine the unstretched flame speed.

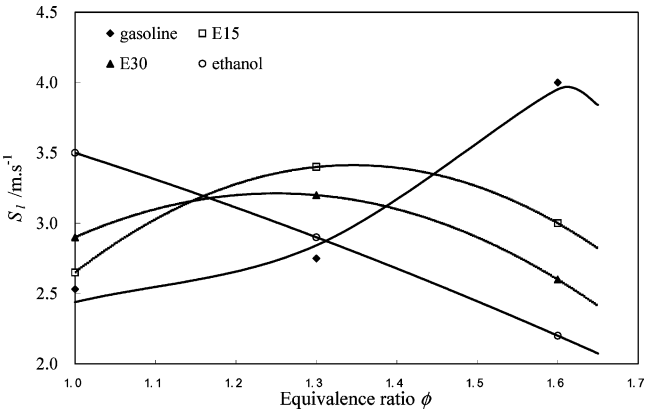

Figure 13. General variation of unstretched flame speeds on the fuel−air ratio.

the combustion pressure, ignition delay time, mass burning rate, and the flame propagation speed are studied in detailed. It is shown that moderate ethanol addition can slightly improve the reliability of a cold start, compared to gasoline, but with the increase of ethane content, this improvement of ethanol on a cold start does not become obvious. Ethanol addition into gasoline results in a significant increase of HC emissions for rich fuel−air mixtures with the same equivalence ratio, but in view of a cold start, it is also indicated that HC and CO emissions can be reduced because the engine can never be overfueled like a gasoline engine.

Acknowledgment. This work is supported by the State Key Project of Fundamental Research Plan, No. 2001CB209208, and supported in part by the Doctorate Foundation of Xi'an Jiaotong University.

Nomenclature

A: Flame area
c_p: Specific heat at constant pressure
c_v: Specific heat at constant volume
h: Enthalpy
Hu: Low heat value
m: Mass
$\dot{m}_b$: Mass burning rate
p: Pressure
Q: Heat loss
R: Gas constant
r_u: Flame radius
S_n: Stretched flame speed
S_l: Unstretched flame speed
t: Elapsed time from ignition
T: Temperature
u: Internal energy
V: Volume
ρ: Density
α: Flame stretch

Subscripts

u: Unburned gas
b: Burned gas
o: Initial condition

EF049733L